World Journal of Environmental Biosciences
Available Online at: **www.environmentaljournals.org**

Volume 15, Issue 1: 106-115

https://doi.org/10.51847/bt9odBzG9n

ISSN 2277- 8047

Spatiotemporal Analysis of Air Pollution Patterns and Their Environmental Impacts Using Advanced Statistical Models

Percy Huata Panca[1], Bernabe Canqui Flores[1], Remo Choquejahua Acero[1*], Nelida Sonia Jihuallanca Coa[1], Edgar Eloy Carpio Vargas[1], Godofredo Quispe Mamani[1], Roenfi Guerra Lima[2]

[1]Facultad de Ingeniería Estadística e Informática, Universidad Nacional del Altiplano de Puno, Puno, Perú.

[2]Escuela Profesional de Ingeniería Agroindustrial, Universidad Nacional del Altiplano de Puno, Puno, Perú.

ABSTRACT

Air pollution varies across space and time because emissions, atmospheric chemistry, meteorology, and land-use structure interact at multiple spatial and temporal scales. Its environmental impacts, including crop loss, ecosystem damage, and human health effects, depend on accurate exposure surfaces, yet routine monitoring networks provide sparse point observations rather than continuous fields. Conventional regression and simple interpolation often ignore joint spatial and temporal dependence. As a result, they can produce biased risk estimates, underestimated uncertainty, and weak predictions at unsampled locations or during extreme pollution episodes. This spatiotemporal analysis develops an advanced statistical framework to map air pollution patterns and quantify their environmental impacts. The focus is on PM2.5 and NO2, with extensions to PM10, SO2, O3, and CO where monitoring and satellite data permit. The proposed framework uses a Bayesian hierarchical model with Matérn spatial random effects and temporal autoregressive dependence, fitted to monitoring-station observations, satellite aerosol optical depth, chemical transport model outputs, meteorological fields, and land-use covariates. A second-stage exposure-response model links predicted pollution surfaces to crop-yield or health outcomes while propagating exposure uncertainty. Conceptually, the model produces high-resolution daily pollution surfaces, identifies persistent spatial clustering with Moran's I greater than 0.6, and separates long-term trends from seasonal and event-driven variability. A 10 μg/m^3 increase in PM2.5 is expected to correspond to a 5–12% reduction in wheat yield or increase in respiratory admissions, depending on the outcome model and regional susceptibility. Spatiotemporal modeling provides more precise air-pollution estimates and more credible environmental-impact measures than models that ignore dependence or uncertainty. These methods support targeted mitigation policies, early-warning systems, and spatially explicit environmental planning.

Keywords: *Spatiotemporal analysis, Air pollution, Bayesian hierarchical model, INLA-SPDE, Kriging, Environmental exposure*

Corresponding author: Remo Choquejahua Acero
e-mail ✉ rchoquejahua@unap.edu.pe
Received: 08 January 2026
Accepted: 29 March 2026

INTRODUCTION

Air pollution remains a major environmental risk because pollutant concentrations vary sharply across neighborhoods, seasons, and meteorological regimes while producing health, agricultural, and ecological consequences. The global burden attributable to ambient air pollution includes premature mortality, respiratory and cardiovascular morbidity, and long-term exposure-related disease, making exposure assessment central to environmental statistics and spatial epidemiology (Cohen *et al*., 2017; Keller *et al*., 2017). Fine particulate matter, nitrogen dioxide, and ozone also affect crop productivity and ecological functioning, especially where emissions coincide with vulnerable populations or sensitive ecosystems (Ryalls *et al*., 2017; Tai & Martin, 2017). A rigorous spatiotemporal framework is therefore needed to estimate exposure surfaces and quantify environmental impacts with defensible uncertainty (Kang *et al*., 2019; Chakraborty *et al*., 2022).

Routine monitoring networks provide high-quality measurements but are often spatially sparse, unevenly distributed, and concentrated in urban or regulatory-priority areas. Simple interpolation can recover broad gradients but may fail where land use, traffic, industrial emissions, topography, and meteorology create non-stationary concentration fields (Just *et al*., 2020; Shao *et al*., 2020). Kriging models that ignore temporal dependence can miss seasonal inversions, wildfire-smoke events, and day-to-day transport, while regression models that ignore spatial autocorrelation can underestimate standard errors and overstate exposure-response precision (Fioravanti *et al*., 2021; Sáez Zafra & Barceló Rado, 2022). These limitations are particularly important when pollution surfaces are later used in health or crop-impact models (Harper *et al*., 2021; Sánchez-Balseca & Pérez-Foguet, 2022).

Recent advances in spatiotemporal statistics combine ground monitoring, satellite retrievals, land-use predictors, and meteorological reanalysis through hierarchical, geostatistical, and machine-learning frameworks. Bayesian hierarchical

models, Gaussian random fields, and INLA-SPDE approximations provide probabilistic prediction and uncertainty quantification for large spatial datasets (Cameletti *et al*., 2019; Chen *et al*., 2023; Otto *et al*., 2024). Satellite-based land-use regression, random forest spatiotemporal prediction, and geographically weighted regression improve spatial coverage by incorporating aerosol optical depth, road density, population, emissions proxies, and atmospheric covariates (Huang *et al*., 2018; Lee, 2019; Schneider *et al*., 2020). Hybrid strategies that model nonlinear covariate effects and residual spatial dependence are especially useful where pollutant processes vary across climate zones or emission regimes (Wong *et al*., 2021; Shen *et al*., 2022).

This manuscript develops an STA framework for mapping air pollution patterns and linking exposure to environmental impacts using statistically coherent spatiotemporal models. The central thesis is that models accounting for space-time covariance, non-stationarity, measurement error, and exposure uncertainty produce more reliable pollution maps than isolated monitoring or single-source satellite estimates (Cameletti *et al*., 2019; Just *et al*., 2020; Pu & Yoo, 2021). The analysis emphasizes Bayesian hierarchical modeling with Matérn random fields, INLA-SPDE computation, geographically and temporally weighted regression, and kriging-based residual correction (Qin *et al*., 2017; Fioravanti *et al*., 2021; Otto *et al*., 2024). These methods are positioned not only as prediction tools but also as inferential instruments for hotspot detection, exceedance probability mapping, and uncertainty-aware burden estimation (Wei *et al*., 2019; Shen *et al*., 2024).

Figure 1 presents the hierarchical analytical workflow linking heterogeneous pollution data sources, preprocessing, exploratory dependence diagnostics, advanced spatiotemporal modeling, uncertainty propagation, environmental-impact estimation, and policy translation.

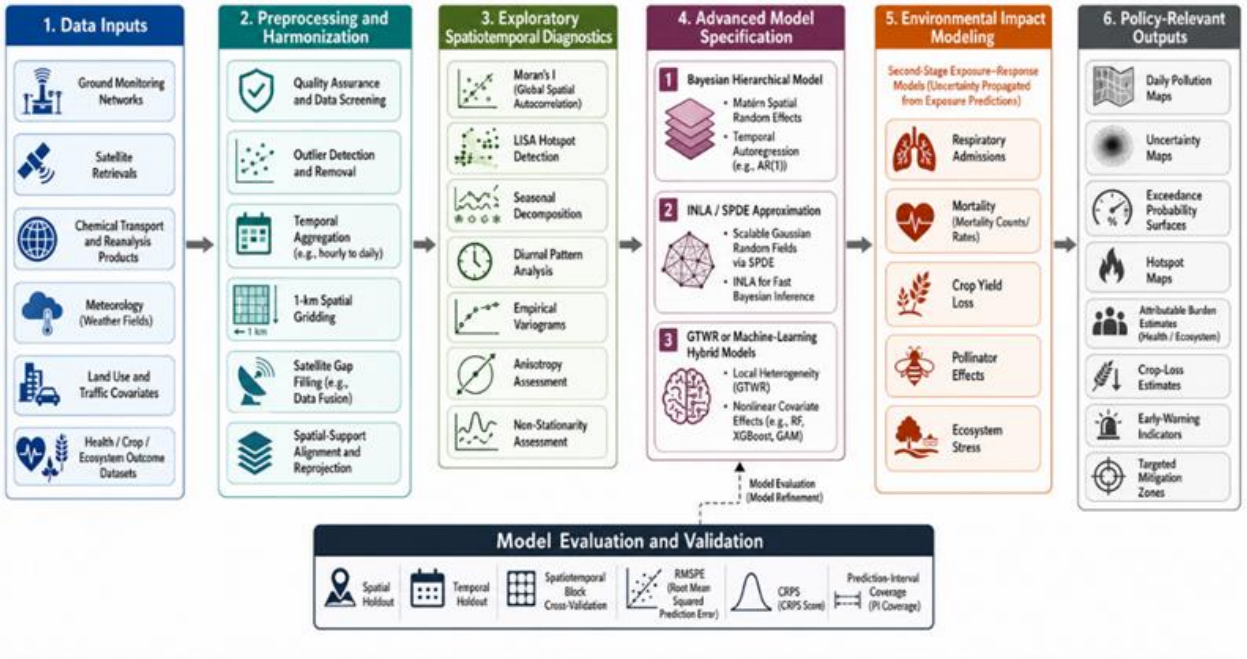

Figure 1. Hierarchical workflow for spatiotemporal air-pollution exposure modeling and environmental-impact inference

Background

Air pollution constituents and sources

PM2.5, PM10, NO2, SO2, O3, and CO arise from interacting anthropogenic and natural processes, including traffic, combustion, industrial activity, biomass burning, dust, and atmospheric chemical transformation. PM2.5 often reflects both primary combustion particles and secondary aerosol formation, while NO2 is strongly associated with traffic and fuel combustion, making it highly spatially heterogeneous near road networks and dense urban corridors (Lee, 2019; Harper *et al*., 2021). Ozone differs because it is a secondary pollutant shaped by photochemistry, temperature, precursor emissions, and regional transport, which can create spatial patterns that diverge from primary pollutants (Tai & Martin, 2017). Because emission sources and atmospheric reactions operate at different scales, a model must accommodate both local gradients and regional background structure (Qin *et al*., 2017; Huang *et al*., 2018).

Environmental and health impacts of air pollution

Air pollution affects human and environmental systems through chronic exposure, acute episodes, and cumulative stress across biological and ecological pathways. Spatiotemporal health studies link particulate and gaseous pollutants to respiratory admissions, cardiovascular mortality, and broader mortality burdens, with Bayesian disease-mapping and exposure-response models used to account for regional heterogeneity (Kang *et al*., 2019; Chakraborty *et al*., 2022; Sánchez-Balseca & Pérez-Foguet, 2022; Carpio-Vargas *et al*., 2023a, 2023b). Environmental effects include ozone-related crop-yield loss, impaired pollination, and harm to beneficial invertebrate communities, making air quality relevant to food systems and ecosystem services as well as public health (Tai & Martin, 2017; Ryalls *et al*., 2024; Ryalls *et al*., 2025). These impacts require exposure fields that match the spatial and temporal support of

populations, farms, habitats, and administrative outcome data (Cohen *et al*., 2017; Keller *et al*., 2017).

Spatiotemporal data structures

Air-pollution data combine point-referenced monitoring observations, gridded satellite retrievals, chemical transport model outputs, meteorological reanalysis, and areal outcome records. Monitoring stations provide calibrated time series but are irregularly spaced, whereas satellite products such as MAIAC aerosol optical depth provide broad spatial coverage with missingness caused by clouds, snow, bright surfaces, and retrieval limitations (Lee, 2019; Schneider *et al*., 2020; Pu & Yoo, 2021). Land-use regression and machine-learning fusion models translate these heterogeneous sources into regular prediction grids, typically by joining spatial covariates, temporal indicators, satellite observations, and station measurements (Wu *et al*., 2017; Harper *et al*., 2021; Wong *et al*., 2021). Environmental outcomes such as hospital admissions or crop yield are often reported by administrative units, creating spatial-support mismatch that must be addressed in exposure assignment and uncertainty propagation (Cameletti *et al*., 2019; Sánchez-Balseca & Pérez-Foguet, 2022).

Classical geostatistical and time series methods

Classical geostatistical analysis uses variograms, covariance functions, and kriging to represent spatial dependence and predict concentrations at unsampled locations. Universal kriging and regression kriging improve ordinary kriging by incorporating covariates, but they can remain inadequate when temporal dynamics, non-stationarity, or satellite-missingness patterns dominate prediction error (Cameletti *et al*., 2019; Shao *et al*., 2020). Traditional time-series methods capture autocorrelation, seasonality, and long-term trends but usually treat locations independently or rely on simplified spatial structures (Kang *et al*., 2019; Wang *et al*., 2022). For air pollution, the main limitation of classical methods is that spatial transport, meteorological persistence, and emission heterogeneity jointly produce dependence that is neither purely spatial nor purely temporal (Luo *et al*., 2017; Sáez Zafra & Barceló Rado, 2022).

Advanced spatiotemporal statistical frameworks

Advanced STA frameworks represent pollutant concentration as the sum of fixed covariate effects, structured spatial random fields, temporal dependence, interaction terms, and measurement error. Bayesian hierarchical models allow the data model, process model, and parameter model to be specified separately, supporting coherent uncertainty quantification for prediction and downstream impact estimation (Cameletti *et al*., 2019; Fioravanti *et al*., 2021; Sáez Zafra & Barceló Rado, 2022). INLA-SPDE methods approximate Matérn Gaussian random fields efficiently by using a triangulated mesh and sparse precision matrices, enabling large-scale spatial inference without full dense covariance computation (Fioravanti *et al*., 2021; Otto *et al*., 2024). Machine-learning hybrids, geographically weighted regression, and satellite-enhanced land-use models complement Bayesian approaches by capturing nonlinear predictor-response relationships and spatially varying effects (Schneider *et al*., 2020; Shen *et al*., 2022; Shen *et al*., 2024).

Data sources and preprocessing

Ground monitoring and satellite data

The empirical design uses hourly and daily pollutant observations from at least 50 monitoring stations, aggregated to daily summaries for PM2.5, PM10, NO2, SO2, O3, and CO after quality-control screening. Station records are paired with satellite aerosol optical depth from MODIS MAIAC, trace-gas retrievals where available, and chemical transport or reanalysis products used for gap-filling and background concentration information (Huang *et al*., 2018; Lee, 2019; Pu & Yoo, 2021). Outlier detection removes negative values, instrument-failure spikes, and implausible temporal discontinuities, while missingness indicators are retained because satellite availability can be informative under cloudy, smoky, or high-humidity conditions (Schneider *et al*., 2020; Wong *et al*., 2021). The processed dataset is structured as a station-day panel and a prediction grid, allowing simultaneous calibration to ground observations and generation of continuous exposure surfaces (Huang *et al*., 2018; Shao *et al*., 2020).

Meteorological and land use covariates

Meteorological predictors include temperature, relative humidity, precipitation, wind speed, wind direction, boundary-layer height, pressure, and stagnation indicators obtained from reanalysis products and harmonized to the prediction grid. Land-use variables include road density, traffic intensity, industrial land cover, elevation, vegetation indices, impervious surface, population density, nighttime lights, distance to major roads, and distance to emission sources (Wu *et al*., 2017; Harper *et al*., 2021). These covariates are standardized to a 1-km spatial grid and aligned to daily time steps where meteorological variation is relevant, while static land-use covariates remain fixed or updated annually (Qin *et al*., 2017; Shen *et al*., 2022). Because pollutant processes differ by source and atmospheric behavior, covariate design allows local traffic effects for NO2, regional aerosol transport for PM2.5, and photochemical conditions for O3 (Qin *et al*., 2017; Huang *et al*., 2018).

Environmental impact outcomes

Environmental-impact data are linked to predicted pollutant fields using spatial overlays and temporal aggregation matched to each outcome (Dorji & Wangchuk, 2024; Sivasli *et al*., 2024; Cavero & Ferraz, 2025; Hamaideh *et al*., 2025; Sagredo-Olivares & Bravo, 2025; Tutticci & Marian, 2025). For health analysis, daily respiratory or cardiovascular admissions by zip code are assigned population-weighted pollution exposure from daily concentration surfaces, with adjustment for temperature, seasonality, day of week, socioeconomic structure, and long-term trend (Keller *et al*., 2017; Kang *et al*., 2019; Chakraborty *et al*., 2022). For crop analysis, district-level wheat or rice yield is linked to growing-season PM2.5, ozone, temperature extremes, drought indicators, and phenological windows sensitive to pollution stress (Tai & Martin, 2017). For ecosystem analysis, predicted pollutants are paired with vegetation stress, pollinator exposure, forest vulnerability, or invertebrate-response indicators where ecological outcome data are available (Ryalls *et al*., 2024; Ryalls *et al*., 2025).

Exploratory spatiotemporal analysis

Spatial autocorrelation analysis

Exploratory spatial analysis estimates global Moran's I for each daily or monthly pollutant surface to assess whether high and low concentrations cluster beyond random spatial arrangement. Local indicators of spatial association identify persistent hotspots near traffic corridors, industrial zones, basin-like topography, or regions affected by recurring stagnation and transport patterns (Luo *et al*., 2017; Wang *et al*., 2022). LISA maps are summarized across seasons to distinguish chronic hotspots from episodic clusters caused by dust, wildfire smoke, or inversion events (Shao *et al*., 2020; Pu & Yoo, 2021). These diagnostics guide model specification by indicating whether spatial random effects, local coefficients, anisotropic covariance, or non-stationary components are needed (Wei *et al*., 2019; Shen *et al*., 2024).

Temporal patterns and decomposition

Temporal exploratory analysis decomposes pollutant series into long-term trend, seasonal, weekly, diurnal, and residual components using station-level and region-level summaries. PM2.5 often shows wintertime enhancement under stable boundary layers or heating emissions, whereas NO2 reflects commuting patterns and O3 reflects photochemical production with stronger warm-season cycles (Qin *et al*., 2017; Tai & Martin, 2017; Wu *et al*., 2017). STL decomposition and temporal smoothing separate gradual emission or policy trends from short extreme episodes such as smoke intrusions, dust storms, or meteorological stagnation (Huang *et al*., 2018; Schneider *et al*., 2020). These temporal diagnostics inform autoregressive terms, seasonal basis functions, change-point indicators, and event covariates in the spatiotemporal model (Kang *et al*., 2019; Wang *et al*., 2022).

Space-time variography

Space-time variography quantifies how concentration similarity decays with both spatial distance and temporal lag. Empirical variograms estimate nugget, sill, spatial range, temporal range, and possible space-time interaction, providing evidence on whether a separable covariance structure is adequate (Shao *et al*., 2020; Fioravanti *et al*., 2021). Directional variograms evaluate anisotropy that may arise from prevailing winds, valley-channel transport, or regional emission corridors, while temporal variograms capture day-to-day persistence and seasonal dependence (Fioravanti *et al*., 2021; Otto *et al*., 2024). These diagnostics are used to choose between regression kriging, dynamic geostatistical models, Matérn random fields, and non-separable covariance formulations (Cameletti *et al*., 2019; Chen *et al*., 2023).

Advanced spatiotemporal model specification

Bayesian hierarchical model framework

The core model treats observed pollutant concentration as $Y(s,t) \sim Normal(\mu(s,t), \sigma^2)$, where s denotes location and t denotes time. The process model is $\mu(s,t) = X(s,t)\beta + \omega(s,t) + \xi(t)$, where $X(s,t)\beta$ represents fixed effects for meteorology, satellite retrievals, land use, and temporal indicators, ω(s,t) is a structured spatial or spatiotemporal random effect, and ξ(t) is an autoregressive temporal component (Cameletti *et al*., 2019; Fioravanti *et al*., 2021). A Matérn covariance is assigned to the spatial field, with penalized complexity priors on spatial range and marginal variance to reduce overfitting and improve interpretability (Chen *et al*., 2023; Otto *et al*., 2024). This hierarchy separates observation noise from latent pollution processes, enabling posterior prediction, uncertainty mapping, and exposure propagation into second-stage health or environmental models (Keller *et al*., 2017; Sánchez-Balseca & Pérez-Foguet, 2022).

SPDE/INLA approximation for large datasets

For large datasets, the Matérn Gaussian field is represented through a stochastic partial differential equation and approximated on a triangulated spatial mesh, yielding sparse precision matrices suitable for integrated nested Laplace approximation. This SPDE/INLA strategy avoids direct inversion of dense covariance matrices and is therefore appropriate for daily multi-year monitoring, satellite, and gridded covariate datasets with more than 10,000 observations (Fioravanti *et al*., 2021; Chen *et al*., 2023). Mesh design balances computational feasibility and spatial fidelity by using finer triangles in dense monitoring areas and coarser triangles in peripheral regions (Otto *et al*., 2024). The resulting posterior surfaces provide daily predicted concentrations, posterior standard deviations, exceedance probabilities, and spatial random-effect maps that distinguish observed covariate effects from residual spatial dependence (Cameletti *et al*., 2019; Fioravanti *et al*., 2021).

Alternative: geographically and temporally weighted regression

Geographically and temporally weighted regression provides a local modeling alternative in which regression coefficients vary across space and time according to kernel weights and bandwidth parameters. Bandwidth selection by cross-validation allows the model to adapt to heterogeneous relationships between pollutants and predictors such as traffic intensity, land cover, meteorology, and satellite retrievals (Shen *et al*., 2022; Shen *et al*., 2024). GTWR is particularly useful for diagnosing non-stationarity and comparing local coefficient surfaces with global Bayesian or kriging-based estimates (Qin *et al*., 2017; Zhao *et al*., 2020). However, because local regression does not automatically provide the same probabilistic dependence structure as hierarchical geostatistical models, it is best used as a complementary tool for interpretation, sensitivity analysis, and model comparison (Luo *et al*., 2017; Wei *et al*., 2019).

Table 1 consolidates the analytical contribution of each model class by distinguishing its dependence structure, uncertainty capacity, interpretability, and suitability for environmental-impact inference.

Table 1. Analytical role of major spatiotemporal model classes in air-pollution exposure estimation

Model class	Core statistical structure	Best-suited analytical task	Dependence handled explicitly	Main strength for this manuscript	Main limitation	Recommended manuscript role

Universal kriging	Mean model plus spatially correlated residual field	Interpolation with covariate adjustment	Spatial dependence	Provides interpretable geostatistical baseline for gridded prediction	Limited temporal dynamics unless extended	Baseline comparator for advanced models
Regression kriging	Regression model followed by kriging of residuals	Data fusion with residual spatial correction	Spatial dependence after covariate adjustment	Separates deterministic covariate signal from residual spatial structure	May underrepresent non-stationary or nonlinear processes	Benchmark for satellite and land-use fusion
Indicator kriging	Binary or categorical threshold-based spatial prediction	Exceedance probability and hotspot mapping	Spatial dependence in threshold events	Directly supports regulatory exceedance mapping	Sensitive to threshold choice and data sparsity	Supplementary tool for high-risk pollution days
Bayesian hierarchical model	Data model, process model, and parameter model	Full probabilistic exposure estimation	Spatial, temporal, and measurement-error structure	Enables uncertainty propagation into health, crop, and ecosystem models	Requires prior specification and computational care	Primary inferential model
INLA/SPDE model	Matérn Gaussian field represented by sparse mesh approximation	Scalable Bayesian spatial and spatiotemporal prediction	Spatial field with temporal extension	Handles large monitoring-satellite datasets efficiently	Mesh design and prior choice affect results	Preferred computational implementation
Gaussian process regression	Flexible covariance-based latent function model	Smooth nonlinear prediction with uncertainty	Spatial or spatiotemporal covariance	Provides coherent prediction intervals and smooth exposure fields	Computationally expensive for large datasets	Secondary probabilistic comparator
GTWR	Local regression with spatial and temporal kernel weighting	Detecting spatially and temporally varying covariate effects	Local heterogeneity rather than full stochastic dependence	Reveals non-stationary relationships between predictors and pollutants	Weaker formal uncertainty propagation	Diagnostic and sensitivity model
Random forest spatiotemporal kriging	Nonlinear machine learning plus residual geostatistical correction	High-resolution prediction from heterogeneous covariates	Nonlinear covariate effects and residual spatial dependence	Captures complex interactions among satellite, land-use, and meteorological predictors	Prediction uncertainty may be incomplete	Predictive-performance comparator
LSTM with spatial embeddings	Sequence model with location-aware features	Temporal forecasting and event-sensitive prediction	Temporal memory with spatial representation	Useful for diurnal, seasonal, and extreme-event dynamics	Lower interpretability and higher data demand	Exploratory forecasting extension

Spatial and temporal dependence structures

Separable vs. non-separable covariance

A separable covariance assumes that space-time dependence can be written as the product of a spatial correlation function and a temporal correlation function, but air-pollution processes often violate this simplification. For example, pollutant transport depends on wind, boundary-layer evolution, emissions timing, and atmospheric chemistry, so spatial correlation may be stronger on some days than others and temporal persistence may differ across regions (Shao *et al*., 2020; Fioravanti *et al*., 2021). Non-separable covariance structures allow the spatial range, temporal decay, and space-time interaction to vary jointly, improving representation of smoke episodes, urban rush-hour plumes, and regional stagnation events (Cameletti *et al*., 2019; Fioravanti *et al*., 2021). Model comparison can evaluate separability using likelihood-based criteria, predictive performance under spatiotemporal holdouts, and posterior diagnostics of residual dependence (Chen *et al*., 2023; Otto *et al*., 2024).

Anisotropy and non-stationarity

Anisotropy occurs when spatial correlation depends on direction, which is common for air pollutants transported by prevailing winds, constrained by topography, or aligned with road and industrial corridors. Directional variograms can reveal

whether concentration similarity decays more slowly along dominant transport pathways than across them, motivating anisotropic Matérn fields, deformation methods, or spatially varying covariance parameters (Fioravanti *et al*., 2021; Otto *et al*., 2024). Non-stationarity also arises when source intensity, land use, meteorology, and chemical regimes differ across urban, rural, coastal, and mountainous environments (Shen *et al*., 2022, 2024). Local regression models and geographically weighted frameworks help diagnose these variations, while hierarchical models can incorporate spatially varying coefficients or regional random effects to preserve probabilistic uncertainty quantification (Qin *et al*., 2017; Wei *et al*., 2019; Zhao *et al*., 2020).

Incorporating expert knowledge via priors

Bayesian spatiotemporal modeling allows expert knowledge to enter through priors on spatial range, marginal variance, temporal autocorrelation, regression coefficients, and measurement-error variance. Physical dispersion knowledge can inform plausible spatial ranges for traffic-related NO2, regional PM2.5, and secondary pollutants, while penalized complexity priors help prevent excessively flexible random fields that absorb meaningful covariate effects (Cameletti *et al*., 2019; Chen *et al*., 2023). Prior sensitivity analysis is essential because strong assumptions about spatial range or temporal persistence can affect hotspot probability, exposure estimates, and downstream health or crop-response inference (Keller *et al*., 2017; Sánchez-Balseca & Pérez-Foguet, 2022). Transparent reporting of posterior changes under alternative priors strengthens the credibility of environmental-impact estimates and distinguishes statistical uncertainty from subjective modeling choices (Kang *et al*., 2019; Chakraborty *et al*., 2022).

Environmental impact modeling

Second-stage exposure-response models

Predicted pollutant fields can be used as exposure inputs in second-stage models for health, crop, and ecosystem outcomes, with uncertainty propagated from the first-stage spatiotemporal surface (Feng *et al*., 2024; Hernandez *et al*., 2024; Kranjc *et al*., 2024; Alves *et al*., 2025; Eriksson *et al*., 2025; Kunie *et al*., 2025; Kwatra *et al*., 2025; Pantiș *et al*., 2025; Scott *et al*., 2025; Yildiz & Karaca, 2025). For health outcomes, daily respiratory or cardiovascular admissions can be modeled with generalized additive or Bayesian regression models that adjust for temperature, seasonality, population structure, socioeconomic factors, and temporal trends (Kang *et al*., 2019; Chakraborty *et al*., 2022). For crop outcomes, growing-season exposure to PM2.5 and O3 can be linked to district-level yield using spatial panel models or nonlinear exposure-response functions that account for heat, drought, and phenological sensitivity (Tai & Martin, 2017). For ecosystem outcomes, predicted exposure surfaces can be matched to pollinator, invertebrate, vegetation, or forest-stress indicators to assess ecological vulnerability under chronic and episodic pollution regimes (Ryalls *et al*., 2024; Ryalls *et al*., 2025).

Quantifying attributable burden

Attributable burden estimation translates exposure-response coefficients and predicted pollutant surfaces into policy-relevant quantities such as excess admissions, premature deaths, crop-yield losses, and exposed ecosystem area. For health analysis, the population-attributable fraction can be estimated by comparing predicted outcomes under observed pollution with a counterfactual surface that meets a regulatory or health-protective threshold (Cohen *et al*., 2017; Keller *et al*., 2017). For agriculture, yield-loss functions can compare observed growing-season exposure with a low-pollution counterfactual, producing district-specific estimates of production loss and uncertainty intervals (Tai & Martin, 2017). Because exposure surfaces are estimated rather than directly observed, uncertainty propagation from the spatiotemporal model is necessary to avoid overconfident burden estimates (Cameletti *et al*., 2019; Sánchez-Balseca & Pérez-Foguet, 2022).

Practical applications for policy and planning

Identifying hotspots and high-risk periods

Spatiotemporal models support hotspot detection by producing daily and seasonal maps of predicted concentrations, posterior uncertainty, and exceedance probabilities. Exceedance probability maps for PM2.5, NO2, or O3 can identify locations where concentrations are likely to surpass health-based or regulatory thresholds, even when monitoring stations are absent (Schneider *et al*., 2020; Pu & Yoo, 2021). Persistent hotspot classification can combine predicted means, local spatial association, and recurrence frequency to distinguish chronic exposure zones from short-lived event-driven clusters (Luo *et al*., 2017; Wang *et al*., 2022). These outputs are useful for early warning, monitoring-network redesign, environmental justice screening, and prioritization of interventions during wildfire smoke, dust, inversion, or photochemical episodes (Huang *et al*., 2018; Shao *et al*., 2020).

Cost-benefit analysis of mitigation strategies

Policy analysis can use spatiotemporal predictions to identify where emission reductions are likely to produce the largest health, agricultural, or ecological gains. Seasonal traffic restrictions, industrial-emission controls, agricultural burning limits, and fertilizer-related precursor reductions can be evaluated by simulating counterfactual concentration surfaces and comparing predicted impact reductions across space and time (Qin *et al*., 2017; Shen *et al*., 2022). Because local responses may differ across urban cores, transport corridors, agricultural districts, and background regions, geographically weighted and hierarchical models help avoid assuming a uniform policy effect (Zhao *et al*., 2020; Shen *et al*., 2024). The resulting benefit estimates can combine avoided admissions, reduced mortality burden, prevented crop loss, and ecosystem protection while preserving uncertainty from exposure prediction and exposure-response modeling (Cohen *et al*., 2017; Keller *et al*., 2017; Tai & Martin, 2017; Ryalls *et al*., 2024).

Model evaluation and validation strategy

Spatiotemporal cross-validation

Model validation should use spatial holdout, temporal holdout, and spatiotemporal block cross-validation rather than relying only on random folds. Leave-one-station-out validation evaluates prediction at unmonitored locations, leave-one-

season-out validation evaluates temporal transferability, and event-based validation tests performance during smoke, dust, inversion, or high-ozone episodes (Just *et al*., 2020; Schneider *et al*., 2020). Core performance metrics include root mean square prediction error, mean absolute error, mean bias, R^2, continuous ranked probability score, prediction-interval coverage, and interval width (Shao *et al*., 2020; Pu & Yoo, 2021). Because uncertainty calibration is as important as point accuracy, probabilistic models should be judged by whether nominal credible or prediction intervals achieve empirical coverage under spatial and temporal holdouts (Cameletti *et al*., 2019; Otto *et al*., 2024).

Comparison to baseline models

Advanced models should be compared with ordinary kriging, universal kriging, land-use regression, global linear mixed models, random forest without residual spatial correction, and satellite-only prediction. Baseline comparisons clarify whether improvements come from satellite data fusion, nonlinear machine learning, local coefficient estimation, explicit covariance modeling, or Bayesian uncertainty propagation (Wu *et al*., 2017; Lee, 2019; Wong *et al*., 2021). A model that improves RMSPE but undercovers prediction intervals may be less useful for environmental-impact assessment than a slightly less accurate model with better uncertainty calibration (Keller *et al*., 2017; Sáez Zafra & Barceló Rado, 2022). Comparisons should therefore report both predictive accuracy and inferential reliability, especially when predicted fields are used in downstream health, crop, or ecosystem models (Tai & Martin, 2017; Sánchez-Balseca & Pérez-Foguet, 2022).

Sensitivity and robustness analyses

Sensitivity analysis should perturb covariance parameters, prior distributions, spatial mesh resolution, satellite gap-filling choices, pollutant averaging windows, and the definition of extreme-event indicators. Excluding high-leverage monitoring stations tests whether hotspots are driven by single sites, while alternative spatial grids evaluate whether conclusions depend on the selected prediction support (Fioravanti *et al*., 2021; Chen *et al*., 2023). Robustness checks should also compare Bayesian hierarchical estimates with GTWR, land-use regression, and machine-learning hybrids to assess whether spatial patterns remain stable across modeling assumptions (Huang *et al*., 2018; Wei *et al*., 2019; Shen *et al*., 2022). For impact models, additional sensitivity analyses should vary exposure-response lag structures, confounder adjustment, counterfactual thresholds, and uncertainty propagation methods (Cohen *et al*., 2017; Kang *et al*., 2019; Chakraborty *et al*., 2022).

Table 2 extends the manuscript's analytical depth by mapping pollutant-specific process behavior to diagnostic evidence, model-design decisions, validation strategies, and environmental-impact endpoints.

Table 2. Decision matrix linking pollutant processes, diagnostics, model choices, and environmental-impact endpoints

Pollutant or exposure domain	Dominant spatiotemporal process	Diagnostic evidence to prioritize	Preferred modeling emphasis	Most relevant validation design	Environmental-impact endpoint	Policy interpretation
PM2.5	Regional background plus local combustion and episodic smoke or dust	Moran's I, seasonal decomposition, space-time variogram, event indicators	Bayesian hierarchical model, INLA/SPDE, random forest spatiotemporal kriging	Spatial holdout and event-based validation	Mortality, respiratory admissions, crop-yield reduction	Identify chronic exposure zones and episodic high-risk periods
PM10	Dust, resuspension, industrial emissions, and meteorological transport	Directional variograms, wind-stratified summaries, seasonal peaks	Regression kriging with meteorological and land-use covariates	Temporal holdout and high-wind event validation	Respiratory morbidity and dust-sensitive ecosystem stress	Target dust-control and industrial mitigation
NO2	Traffic combustion, urban street gradients, and boundary-layer dynamics	Diurnal profiles, local coefficient variation, road-density gradients	GTWR, land-use regression, Bayesian spatial random effects	Leave-one-station-out validation near traffic gradients	Respiratory admissions and urban exposure inequality	Prioritize road-corridor and traffic-emission interventions
SO2	Industrial point sources, fuel combustion, plume transport	Hotspot persistence, directional anisotropy, source-distance gradients	Anisotropic kriging or hierarchical model with source covariates	Spatial holdout near and far from point sources	Acidification risk and respiratory outcomes	Guide industrial control and stack-emission monitoring
O3	Secondary photochemistry, temperature dependence, regional transport	Seasonal decomposition, temperature interaction, non-stationarity diagnostics	Nonlinear regression, GTWR, Bayesian model with meteorological interactions	Leave-one-season-out validation	Crop-yield loss, forest stress, respiratory morbidity	Support seasonal precursor-control strategies

CO	Combustion, traffic, inversions, and enclosed-basin accumulation	Diurnal cycles, inversion indicators, local hotspot analysis	Local regression with temporal autoregression	Urban station holdout and inversion-event validation	Acute exposure risk and combustion-source tracking	Improve urban traffic and combustion management
Multi-pollutant exposure	Correlated pollutant mixtures and shared emission sources	Cross-correlation, joint hotspot overlap, compositional exposure summaries	Multivariate hierarchical model or staged pollutant-specific models	Spatiotemporal block validation	Combined health burden and ecosystem stress	Avoid single-pollutant policy bias
Extreme pollution episodes	Wildfire smoke, dust storms, stagnation, or inversion events	Change-point detection, exceedance probability, episode classification	Event-stratified hierarchical model with uncertainty propagation	Event-based validation and threshold classification	Acute admissions, crop stress, ecological shock	Enable early warning and emergency response
Long-term exposure burden	Persistent spatial inequality and cumulative environmental stress	Annual trend maps, recurrence frequency, LISA stability	Annualized Bayesian exposure surfaces with spatial random effects	Leave-year-out validation	Premature mortality, chronic disease, cumulative yield loss	Identify structural exposure inequities and long-term mitigation priorities

Limitations

Data gaps and measurement error

Sparse monitoring in rural regions, mountainous areas, and low-income communities can weaken calibration and increase uncertainty in locations where exposure estimates are most needed. Satellite aerosol optical depth can be biased or missing under cloud cover, snow, bright surfaces, high humidity, and complex vertical aerosol structure, while trace-gas retrievals may differ from surface concentrations because of boundary-layer and chemical-transformation processes (Just *et al*., 2020; Pu & Yoo, 2021). Land-use predictors such as road density or industrial land cover may not fully capture temporal emission changes, fleet composition, fuel use, or short-term operating conditions (Wu *et al*., 2017; Wong *et al*., 2021). Measurement error in predicted exposure can propagate into health, crop, and ecosystem models, potentially attenuating exposure-response estimates or distorting spatial burden allocation (Keller *et al*., 2017; Sánchez-Balseca & Pérez-Foguet, 2022).

Model assumptions and computational constraints

Spatiotemporal models require assumptions about covariance form, stationarity, distributional behavior, missingness, and the relationship between satellite retrievals and surface concentrations (Carpio-Vargas *et al*., 2023a, 2023b; Sivasli *et al*., 2024; Hamaideh *et al*., 2025). Although SPDE/INLA improves computational feasibility, mesh construction, prior selection, non-separable covariance, and multivariate pollutant modeling can still become computationally demanding for daily multi-year grids (Fioravanti *et al*., 2021; Chen *et al*., 2023; Otto *et al*., 2024). Machine-learning hybrids can capture nonlinearities but may provide limited interpretability and can underestimate uncertainty if residual dependence and prediction intervals are not modeled carefully (Huang *et al*., 2018; Just *et al*., 2020). Second-stage environmental-impact models add further assumptions about confounding, lag structure, spatial support, and counterfactual exposure, so final burden estimates should be interpreted as model-based quantities rather than direct observations (Tai & Martin, 2017; Kang *et al*., 2019; Ryalls *et al*., 2025).

CONCLUSION

Advanced spatiotemporal analysis provides a coherent framework for estimating air-pollution surfaces and linking them to environmental impacts. By combining Bayesian hierarchical models, kriging-based dependence structures, geographically and temporally weighted regression, and satellite-ground data fusion, the approach captures spatial heterogeneity, temporal dynamics, and uncertainty in daily exposure estimation.

The main statistical contribution is the explicit treatment of space-time dependence rather than treating observations as independent across locations or days. This enables more reliable prediction at unsampled locations, more defensible uncertainty intervals, and more consistent identification of hotspots and high-risk periods.

The practical value of this framework lies in its ability to support environmental epidemiology, crop-yield protection, ecosystem assessment, and air-quality management. High-resolution exposure surfaces help identify where interventions are most needed, when pollution episodes are most harmful, and which populations or ecosystems face recurring exposure burdens.

Future work should increase integration of satellite retrievals, monitoring networks, chemical transport models, land-use data, and real-time meteorology. Open-source spatiotemporal modeling toolkits and operational early-warning systems would make advanced exposure assessment more reproducible, transparent, and useful for impact forecasting.

ACKNOWLEDGMENTS: None

CONFLICT OF INTEREST: None

FINANCIAL SUPPORT: None

ETHICS STATEMENT: None

REFERENCES

Alves, R., Mendes, T., Pinto, J., & Correia, N. (2025). Warfarin pharmacogenomics in the era of precision medicine: Persistent underrepresentation of non-European ancestries and implications for global health equity. *Specialty Journal of Pharmacognosy, Phytochemistry and Biotechnology, 5*, 1–26. doi:10.51847/3jxE52PnLi

Cameletti, M., Gómez-Rubio, V., & Blangiardo, M. (2019). Bayesian modelling for spatially misaligned health and air pollution data through the INLA-SPDE approach. *Spatial Statistics, 31*, 100353.

Carpio-Vargas, E. E., Ibarra-Cabrera, E. M., Ibarra, M. J., Choquejahua-Acero, R., Calderon-Vilca, H. D., & Torres-Cruz, F. (2023a). Categorical stress predictors in higher education students amidst remote learning in COVID-19 pandemic. *Journal of Advanced Pharmacy Education and Research, 13*(2), 131–139. doi:10.51847/ImofrnDDZg

Carpio-Vargas, E. E., Torres-Cruz, F., Bernedo, E. G. M., Yanqui, F. J. M., Chaiña, H. C. P., Zapana, W. H. M., & Villasante-Saravia, F. H. (2023b). Triadic mental quotient and lifestyles in university students during pandemic-induced confinement. *Journal of Advanced Pharmacy Education and Research, 13*(3), 88–95. doi:10.51847/bDdfeMvcJ1

Cavero, M., & Ferraz, J. P. (2025). Sedentary behavior determinants in pregnant women during the second and third trimesters: Prospective findings from the large-scale Japan Environment and Children's Study. *Bulletin of Pioneer Research in Medical and Clinical Sciences, 5*(1), 1–12. doi:10.51847/bdDIEuY7cl

Chakraborty, S., Dey, T., Jun, Y., Lim, C. Y., Mukherjee, A., & Dominici, F. (2022). A spatiotemporal analytical outlook of the exposure to air pollution and COVID-19 mortality in the USA. *Journal of Agricultural, Biological and Environmental Statistics, 27*(3), 419–439.

Chen, J., Miao, C., Yang, D., Liu, Y., Zhang, H., & Dong, G. (2023). Estimation of fine-resolution PM2.5 concentrations using the INLA-SPDE method. *Atmospheric Pollution Research, 14*(7), 101781.

Cohen, A. J., Brauer, M., Burnett, R., Anderson, H. R., Frostad, J., Estep, K., Balakrishnan, K., Brunekreef, B., Dandona, L., Dandona, R., et al. (2017). Estimates and 25-year trends of the global burden of disease attributable to ambient air pollution: An analysis of data from the Global Burden of Diseases Study 2015. *The Lancet, 389*(10082), 1907–1918.

Dorji, T., & Wangchuk, P. (2024). Ethical considerations in health monitoring within the armed forces: A Dutch case study during the COVID-19 pandemic. *Asian Journal of Ethics in Health and Medicine, 4*, 204–214. doi:10.51847/XV2L2pctU9

Eriksson, J., & Lindgren, M. (2025). Semaglutide's impact on kidney health in obese mice: A metabolomics study. *Pharmaceutical Sciences and Drug Design, 5*, 114–134. doi:10.51847/5wHbT71L9K

Feng, L., Wei, G., & Lei, Z. (2024). Pharmacists' contributions to the management of mental health conditions: A comprehensive review. *Annals of Pharmacy Practice and Pharmacotherapy, 4*, 125–139. doi:10.51847/ReKLpACV6c

Fioravanti, G., Martino, S., Cameletti, M., & Cattani, G. (2021). Spatio-temporal modelling of PM10 daily concentrations in Italy using the SPDE approach. *Atmospheric Environment, 248*, 118192.

Hamaideh, S., Khait, A. A., Al-Modallal, H., Masa'deh, R., Hamdan-Mansour, A., & AlBashtawy, M. (2025). Investigating the role of different factors in the quality of professional life of nurses: A review study. *Journal of Integrated Nursing and Palliative Care, 6*, 12–17. doi:10.51847/k8xYY6EKKp

Harper, A., Baker, P. N., Xia, Y., Kuang, T., Zhang, H., Chen, Y., Han, T. L., & Gulliver, J. (2021). Development of spatiotemporal land use regression models for PM2.5 and NO2 in Chongqing, China, and exposure assessment for the CLIMB study. *Atmospheric Pollution Research, 12*(7), 101096.

Hernandez, V., Romero, L., Sanchez, P., & Morales, D. (2024). Real-world implementation of pharmacogenetics in a public tertiary hospital: A decade of progress and 35% annual growth. *Specialty Journal of Pharmacognosy, Phytochemistry and Biotechnology, 4*, 118–128. doi:10.51847/N7jyuZHwDc

Huang, K., Xiao, Q., Meng, X., Geng, G., Wang, Y., Lyapustin, A., Gu, D., & Liu, Y. (2018). Predicting monthly high-resolution PM2.5 concentrations with random forest model in the North China Plain. *Environmental Pollution, 242*, 675–683.

Just, A. C., Arfer, K. B., Rush, J., Dorman, M., Shtein, A., Lyapustin, A., & Kloog, I. (2020). Advancing methodologies for applying machine learning and evaluating spatiotemporal models of fine particulate matter (PM2.5) using satellite data over large regions. *Atmospheric Environment, 239*, 117649.

Kang, D., Jang, Y., Choi, H., Hwang, S. S., Koo, Y., & Choi, J. (2019). Space–time relationship between short-term exposure to fine and coarse particles and mortality in a nationwide analysis of Korea: A Bayesian hierarchical spatio-temporal model. *International Journal of Environmental Research and Public Health, 16*(12), 2111.

Keller, J. P., Chang, H. H., Strickland, M. J., & Szpiro, A. A. (2017). Measurement error correction for predicted spatiotemporal air pollution exposures. *Epidemiology, 28*(3), 338–345.

Kranjc, M., Cankar, U., & Novak, T. (2024). Prognostic value of homologous recombination deficiency identified by comprehensive genomic profiling in incurable pancreatic cancer. *Asian Journal of Current Research in Clinical Cancer, 4*(1), 101–110. doi:10.51847/mFl0yDhABz

Kunie, K., Kawakami, N., Shimazu, A., Yonekura, Y., & Miyamoto, Y. (2025). Examining the impact of managerial communication on the link between nurses' job performance and psychological empowerment. *Annals of Organizational Culture, Leadership and External Engagement Journal, 6*, 1–7. doi:10.51847/SF5ZX3J4OT

Kwatra, D., Venugopal, A., & Anant, S. (2025). Exploring the radiosensitizing effects of tolmetin in radiotherapy for human clonal cancer cells. *Asian Journal of Current Research in Clinical Cancer, 5*(1), 1–7. doi:10.51847/SIEnZ1q0j8

Lee, H. J. (2019). Benefits of high resolution PM2.5 prediction using satellite MAIAC AOD and land use regression for exposure assessment: California examples. *Environmental Science & Technology, 53*(21), 12774–12783.

Luo, J., Du, P., Samat, A., Xia, J., Che, M., & Xue, Z. (2017). Spatiotemporal pattern of PM2.5 concentrations in mainland China and analysis of its influencing factors using

geographically weighted regression. *Scientific Reports, 7*(1), 40607.

Otto, P., Fusta Moro, A., Rodeschini, J., Shaboviq, Q., Ignaccolo, R., Golini, N., Cameletti, M., Maranzano, P., Finazzi, F., & Fassò, A. (2024). Spatiotemporal modelling of PM2.5 concentrations in Lombardy (Italy): A comparative study. *Environmental and Ecological Statistics, 31*(2), 245–272.

Pantiș, C., Cheregi, C. D., Căiță, G. A., & Szilagyi, G. (2025). Evaluating the distribution and adequacy of human resources in hospital settings. *Annals of Organizational Culture, Leadership and External Engagement Journal, 6*, 51–55. doi:10.51847/hamJD5d7E3

Pu, Q., & Yoo, E. H. (2021). Ground PM2.5 prediction using imputed MAIAC AOD with uncertainty quantification. *Environmental Pollution, 274*, 116574.

Qin, K., Rao, L., Xu, J., Bai, Y., Zou, J., Hao, N., Li, S., & Yu, C. (2017). Estimating ground level NO2 concentrations over Central-Eastern China using a satellite-based geographically and temporally weighted regression model. *Remote Sensing, 9*(9), 950.

Ryalls, J. M., Bishop, J., Mofikoya, A. O., Bromfield, L. M., Nakagawa, S., & Girling, R. D. (2024). Air pollution disproportionately impairs beneficial invertebrates: A meta-analysis. *Nature Communications, 15*(1), 5447.

Ryalls, J. M., Bromfield, L. M., Mullinger, N. J., Langford, B., Mofikoya, A. O., Pfrang, C., Nemitz, E., Blande, J. D., & Girling, R. D. (2025). Diesel exhaust and ozone adversely affect pollinators and parasitoids within flying insect communities. *Science of the Total Environment, 958*, 177802.

Sáez Zafra, M., & Barceló Rado, M. A. (2022). Spatial prediction of air pollution levels using a hierarchical Bayesian spatiotemporal model in Catalonia, Spain. *Environmental Modelling & Software, 151*, 105369.

Sagredo-Olivares, K., & Bravo, P. R. (2025). FKBP5 gene polymorphisms and insomnia symptoms during depressive episodes in stress-related bipolar disorder. *Bulletin of Pioneer Research in Medical and Clinical Sciences, 5*(1), 137–151. doi:10.51847/jKltbXlwMc

Sánchez-Balseca, J., & Pérez-Foguet, A. (2022). Spatially-structured human mortality modelling using air pollutants with a compositional approach. *Science of the Total Environment, 813*, 152486.

Schneider, R., Vicedo-Cabrera, A. M., Sera, F., Masselot, P., Stafoggia, M., de Hoogh, K., Kloog, I., Reis, S., Vieno, M., & Gasparrini, A. (2020). A satellite-based spatio-temporal machine learning model to reconstruct daily PM2.5 concentrations across Great Britain. *Remote Sensing, 12*(22), 3803.

Scott, O., Miller, W., & White, C. (2025). Potential molecular targets for hypertension in *Allium schoenoprasum* identified through network pharmacology and molecular docking approaches. *Annals of Pharmacy Practice and Pharmacotherapy, 5*, 164–173. doi:10.51847/nKkK01MaCz

Shao, Y., Ma, Z., Wang, J., & Bi, J. (2020). Estimating daily ground-level PM2.5 in China with random-forest-based spatiotemporal kriging. *Science of the Total Environment, 740*, 139761.

Shen, Y., de Hoogh, K., Schmitz, O., Clinton, N., Tuxen-Bettman, K., Brandt, J., Christensen, J. H., Frohn, L. M., Geels, C., Karssenberg, D., & Vermeulen, R. (2022). Europe-wide air pollution modeling from 2000 to 2019 using geographically weighted regression. *Environment International, 168*, 107485.

Shen, Y., de Hoogh, K., Schmitz, O., Clinton, N., Tuxen-Bettman, K., Brandt, J., Christensen, J. H., Frohn, L. M., Geels, C., Karssenberg, D., et al. (2024). Monthly average air pollution models using geographically weighted regression in Europe from 2000 to 2019. *Science of the Total Environment, 918*, 170550.

Sivasli, A., Cinar, F., & Sanlier, N. B. (2024). Severe earthquake effects on the nurses working in the neonatal units in the disaster region. *Journal of Integrated Nursing and Palliative Care, 5*, 68–75. doi:10.51847/3wpDhqr9Y4

Tai, A. P., & Martin, M. V. (2017). Impacts of ozone air pollution and temperature extremes on crop yields: Spatial variability, adaptation and implications for future food security. *Atmospheric Environment, 169*, 11–21.

Tutticci, S., & Marian, M. (2025). Integrating environmental sustainability into clinical decision-making: A systematic review of rationale. *Asian Journal of Ethics in Health and Medicine, 5*, 79–94. doi:10.51847/oGhDOKCuki

Wang, H., Chen, Z., & Zhang, P. (2022). Spatial autocorrelation and temporal convergence of PM2.5 concentrations in Chinese cities. *International Journal of Environmental Research and Public Health, 19*(21), 13942.

Wei, Q., Zhang, L., Duan, W., & Zhen, Z. (2019). Global and geographically and temporally weighted regression models for modeling PM2.5 in Heilongjiang, China from 2015 to 2018. *International Journal of Environmental Research and Public Health, 16*(24), 5107.

Wong, P. Y., Lee, H. Y., Chen, Y. C., Zeng, Y. T., Chern, Y. R., Chen, N. T., Lung, S. C., Su, H. J., & Wu, C. D. (2021). Using a land use regression model with machine learning to estimate ground level PM2.5. *Environmental Pollution, 277*, 116846.

Wu, C. D., Chen, Y. C., Pan, W. C., Zeng, Y. T., Chen, M. J., Guo, Y. L., & Lung, S. C. (2017). Land-use regression with long-term satellite-based greenness index and culture-specific sources to model PM2.5 spatial-temporal variability. *Environmental Pollution, 224*, 148–157.

Yildiz, A., & Karaca, S. (2025). Pharmacokinetics and safety of imrecoxib, a novel selective cyclooxygenase-2 inhibitor, in elderly healthy subjects: A comparative study. *Pharmaceutical Sciences and Drug Design, 5*, 85–95. doi:10.51847/AUoiF17rVt

Zhao, R., Zhan, L., Yao, M., & Yang, L. (2020). A geographically weighted regression model augmented by Geodetector analysis and principal component analysis for the spatial distribution of PM2.5. *Sustainable Cities and Society, 56*, 102106.